LYMPHATIC RESEARCH AND BIOLOGY
Volume 10, Number 4, 2012

DOI: 10.1089/lrb.2012.0014

Relationships Between Lymphangiogenesis and Angiogenesis During Inflammation in Rat Mesentery Microvascular Networks

Richard S. Sweat, Peter C. Stapor, and Walter L. Murfee, Ph.D.

Abstract

Background: Lymphatic and blood microvascular systems play a coordinated role in the regulation of interstitial fluid balance and immune cell trafficking during inflammation. The objective of this study was to characterize the temporal and spatial relationships between lymphatic and blood vessel growth in the adult rat mesentery following an inflammatory stimulus.

Methods and Results: Mesenteric tissues were harvested from unstimulated adult male Wistar rats and at 3, 10, and 30 days post compound 48/80 stimulation. Tissues were immunolabeled for PECAM, LYVE-1, Prox1, podoplanin, CD11b, and class III β-tubulin. Vascular area, capillary blind end density, and vascular length density were quantified for each vessel system per time point. Blood vascular area increased compared to unstimulated tissues by day 10 and remained increased at day 30. Following the peak in blood capillary sprouting at day 3, blood vascular area and density increased at day 10. The number of blind-ended lymphatic vessels and lymphatic density did not significantly increase until day 10, and lymphatic vascular area was not increased compared to the unstimulated level until day 30. Lymphangiogenesis correlated with the upregulation of class III β-tubulin expression by endothelial cells along lymphatic blind-ended vessels and increased lymphatic/blood endothelial cell connections. In local tissue regions containing both blood and lymphatic vessels, the presence of lymphatics attenuated blood capillary sprouting.

Conclusions: Our work suggests that lymphangiogenesis lags angiogenesis during inflammation and motivates the need for future investigations aimed at understanding lymphatic/blood endothelial cell interactions. The results also indicate that lymphatic endothelial cells undergo phenotypic changes during lymphangiogenesis.

Introduction

Blood and lymphatic microvascular networks play critical roles in the trafficking of leukocytes and the clearance of excess fluid from local tissue spaces.[1] Given the importance of these dynamics in inflammation, wound repair, tumor metastasis, lymphedema, and other pathological conditions, understanding the coordination between the lymphatic and blood vascular systems is critical. New insights can be gained by elucidating the relationships between angiogenesis, defined as the growth of new blood vessels from existing ones, and lymphangiogenesis, defined as the analogous growth of new lymphatic vessels.

During inflammation and wound healing scenarios, lymphangiogenesis has been reported to lag angiogenesis.[2,3] In another study, Benest et al. showed that the presence of lymphatic vessels could influence the level of angiogenesis post VEGF-C stimulation.[4] These results identify fundamental temporal and spatial relationships between lymphangiogenesis and angiogenesis and motivate similar types of studies using alternative models. The objective of this study was to characterize the temporal and spatial relationships between lymphatic and blood vessel growth following an inflammatory stimulus in the adult rat mesentery. The rat mesentery was selected because it provides an *en face* view of an entire microvascular network down to a single cell level. We show that, while mast cell degranulation via compound 48/80 causes both angiogenesis and lymphangiogenesis, lymphatic growth lags blood capillary sprouting and that the local presence of lymphatic vessels attenuates angiogenesis. Our results also indicate that a change in the local environment can cause an increase in physical lymphatic/blood endothelial cell connections. Finally, the value of characterizing growth responses over a time course is exemplified by our discovery of a

Department of Biomedical Engineering, Tulane University, New Orleans, Louisiana.

potential phenotypic marker for lymphatic endothelial cells during lymphangiogenesis.

Material and Methods

Mast cell degranulation model

All experiments were performed in accordance with the guidelines of the Tulane University Institutional Animal Care and Use Committee. Similar to previously established protocols,[5–7] single 2.5 mL doses of compound 48/80 (140, 280, 420, 560, and 700 μg/mL in saline) were administered by intraperitoneal injection over the course of 3 days (twice a day and once on the final day) in increasing concentrations into 350–450 g adult male Wistar rats. Mesenteric tissue windows, defined as the thin translucent connective tissues attached to small intestine, were harvested according to the following experimental groups: Unstimulated ($n=4$ animals) and 3 days ($n=4$ animals), 10 days ($n=4$ animals), and 30 days ($n=4$ animals) after stimulation with compound 48/80. This model was used for the current study because it has been shown to produce a robust angiogenic response across the hierarchy of microvascular networks over a relatively short time course.[8,9]

Tissue harvesting and immunohistochemistry

At the time of harvesting, animals were anesthetized by intramuscular injection of ketamine (80 mg/kg bw) and xylazine (8 mg/kg bw). Following anesthesia, animals were euthanized by intracardiac injection of Beuthanasia. The mesentery was surgically exposed and 12 mesenteric windows were harvested starting from the ileum. Tissues were whole mounted on glass slides, fixed in methanol for 30 min at −20°C, and washed every 10 min for 30 min with phosphate-buffered saline (PBS) containing 0.1% saponin. Tissues were then labeled with combinations of antibodies to LYVE-1, PECAM (CD31), Prox1, podoplanin, CD11b, or class III β-tubulin. LYVE-1 and PECAM/Prox1/podoplanin/CD11b labeling protocol: 1) 1 h incubation at room temperature with 1:100 rabbit polyclonal LYVE-1 antibody (AngioBio, Del Mar, CA), one of the following: 1:200 mouse monoclonal biotinylated CD31 antibody (BD Pharmingen, San Diego, CA), 1:100 mouse monoclonal Prox1 antibody (Novus Biologicals, Littleton, CO), 1:50 mouse monoclonal podoplanin antibody (AngioBio), or 1:100 mouse monoclonal CD11b antibody (AbD Serotec, Raleigh, NC), and 5% normal goat serum (NGS) (Jackson ImmunoResearch Laboratories, West Grove, PA); 2) 1 h incubation at room temperature with 1:100 goat anti-rabbit CY2-conjugated antibody (Jackson ImmunoResearch Laboratories), CY3-conjugated streptavidin secondary (Jackson ImmunoResearch Laboratories), and 5% NGS. Class III β-tubulin and PECAM/LYVE-1/Prox1 labeling protocol: 1) 36 h incubation at 4°C with 1:200 mouse monoclonal class III β-tubulin antibody (2G10, Abcam, Cambridge, MA) and 5% NGS; 2) 36 h incubation at 4°C with 1:100 goat anti-mouse CY2-conjugated secondary antibody and 5% NGS; 3) 1 h incubation at room temperature with 5% normal mouse serum (Jackson ImmunoResearch Laboratories) (for PECAM); 4) 1 h incubation at room temperature with antibodies to either PECAM or LYVE-1, as described above, or 1:100 rabbit polyclonal Prox1 antibody (Novus Biologicals); 5) 1 h incubation at room temperature with CY3-conjugated streptavidin secondary or 1:100 goat anti-rabbit CY3-conjugated antibody (Jackson ImmunoResearch Laboratories). All antibodies were diluted in antibody buffer (0.1% saponin in PBS + 2% bovine serum albumin). All steps were followed by washes every 10 min for 30 min with PBS containing 0.1% saponin. Positive antibody labeling was confirmed by comparisons with unstained, secondary antibody alone, or IgG plus secondary antibody labeled control groups.

Quantification of lymphangiogenesis, angiogenesis, and lymphatic/blood endothelial cell connections in microvascular networks

Immunolabeled tissues were imaged on an Olympus IX70 inverted fluorescence microscope coupled with a Photometrics CoolSNAP EZ camera using 4× dry, 10× dry, 20× dry, 20× oil, and 60× oil objectives, an inverted Zeiss LSM 510 confocal microscopy system using a 63× oil objective, or a Nikon A1 confocal microscopy system using a 60× oil objective. Tissues containing both blood and lymphatic vessels were randomly selected for analysis per experimental group: unstimulated ($n=7$ tissues; 1–2 tissues × 4 animals), day 3 post stimulation ($n=7$ tissues; 1–2 tissues × 4 animals), day 10 post stimulation ($n=7$ tissues; 1–2 tissues × 4 animals), and day 30 post stimulation ($n=8$ tissues; 2 tissues × 4 animals). Blood and lymphatic vessels were quantified based on PECAM or LYVE-1 labeling, respectively. The following metrics were quantified from montages of entire tissues generated from images captured using the 4× objective: blood vascular area per tissue area, lymphatic vascular area per tissue area, the number of blood capillary blind ends per vascular area, the number of lymphatic blind ends per vascular area, blood vessel length per vascular area, lymphatic vessel length per vascular area, and lymphatic/blood endothelial cell connections. Lymphatic and blood vascular area was defined as the sum of the areas circumscribed by the perimeter of each respective vessel network type. Blind ends were defined as blind-ended blood or lymphatic capillaries extending from a network. The effect of the lymphatic vessel presence on angiogenesis was investigated by quantifying the number of blood capillary blind ends in local areas in a tissue with or without lymphatic vessels. Lymphatic/blood endothelial cell connections were identified based on 1) continuous PECAM labeling across blood and lymphatic endothelial cells at connection sites, and 2) a shared endothelial cell morphology.[10] Vascular length density was measured on two 4x fields of view randomly selected from each tissue. All measurements were performed using ImageJ version 1.44p (ImageJ, U.S. National Institutes of Health, Bethesda, ML).

In an additional analysis, the number of blood capillary blind ends per vascular area was compared between tissues with lymphatic vessels ($n=7$ tissues, 1–2 tissues × 4 rats) versus tissues without lymphatic vessels ($n=4$ tissues, 2 tissues × 2 rats).

Intraluminal labeling of blood vessels at locations of lymphatic/blood endothelial cell connections

A 2 mL bolus of 40 kDa lysine-fixable FITC-dextran (10 mg/mL, Molecular Probes, Eugene, OR) was injected via the femoral vein of anesthetized animals. Animals were then euthanized and the mesenteric tissue fixed by soaking the intraperitoneal space with 4% paraformaldehyde for 1 h. Mesenteric tissue windows were then harvested, mounted, and labeled for PECAM as described above.

Statistical analysis

Comparisons for angiogenic and lymphangiogenic metrics were analyzed across the time course of the compound 48/80 mast cell degranulation model using a one-way ANOVA followed by a Student-Newman-Keuls pairwise comparison test (SigmaStat; Systat Software, Inc., Chicago, IL). Two group comparisons were analyzed using a Student's *t*-test. Statistical significance was accepted for $p < 0.05$. Values are presented as means ± standard error of the means.

Results

Lymphatic Vessel Growth is Delayed Compared to Blood Vessel Growth

Compound 48/80-induced mast cell degranulation resulted in dramatic blood microvascular network growth (Figs. 1 and 2). The inflammatory stimulus also caused dramatic lymphatic network growth (Figs. 1 and 2). Growth in both systems was characterized by increases in capillary sprouting associated with increases in vessel density and network area (Fig. 2). Blood and lymphatic microvessels across the hierarchy of microvascular networks were labeled positively for PECAM. Lymphatic vessels were distinguished from blood vessels based upon a decreased PECAM labeling intensity, a discontinuous labeling pattern,[3,11] and positive LYVE-1 expression. LYVE-1 labeling co-localized with podoplanin and identified all Prox-1 positive lymphatic vessels (Fig. 3E–3J). Angiogenesis was evident in blood microvascular networks at day 3 by the increased number of blind-ended capillary sprouts (Fig. 2F). At day 10, blood capillary sprouting remained elevated and returned to unstimulated levels by day 30. The increase in sprouting at day 3 preceded increases in blood vascular area and density at day 10 (Fig. 2E and 2G). By day 30, blood vascular area remained increased compared to unstimulated levels, yet vascular density had decreased compared to day 10. An increase in the number of lymphatic blind-ended vessels, indicative of lymphangiogenesis, did not occur until day 10 (Fig. 2I). The number of lymphatic blind ends remained elevated at day 30. Lymphatic capillary sprouting at day 10 and day 30 was further supported by the observation of LYVE-1 positive endothelial filopodia extensions off of existing vessels (Fig. 3C and 3D). Also, the morphology of lymphatic blind ends was commonly more tapered and less blunt-ended than the unstimulated and day 3 groups. As another indicator of lymphangiogenesis, lymphatic sprouting was accompanied by an increase in apparent intussusceptive loops (data not shown). Lymphatic vessel density increased compared to the unstimulated level by day 10 (Fig. 2J). At day 30, lymphatic vessel density remained elevated and was associated with an increase in lymphatic network area (Fig. 2H). At days 3, 10, and 30 post stimulation, LYVE-1 labeling identified a subpopulation of CD11b positive interstitial cells (Fig. 4). Based on qualitative observation, LYVE-1 positive interstitial cells were CD11b positive, indicating that these cells could be activated macrophages.

Presence of lymphatic vessels attenuates angiogenesis

In order to further investigate the local influence of lymphatic vessels on angiogenesis, we also analyzed blood capillary sprouting outside and inside regions of overlapping lymphatic and blood vascular networks. This allowed for the comparison of blood capillary sprouting in local regions with no lymphatic vessels versus regions with lymphatic vessels (Fig. 5). In blood vessel only regions, capillary sprouting was dramatically increased at day 3 compared to unstimulated networks (Fig. 5A). Capillary sprouting remained increased at day 10 and returned to unstimulated levels by day 30. In contrast, blood capillary sprouting in regions with lymphatic vessels did not increase over the 30 day time course (Fig. 5B). At day 3, blood capillary sprouting in local regions with lymphatics was attenuated versus regions without lymphatics (Fig. 5C). This result is supported by the comparison of capillary sprouting at the same time point between tissues with and without lymphatic vessels (Fig. 5C). Both comparisons suggest that the presence of lymphatic vessels influences inflammation induced angiogenesis.

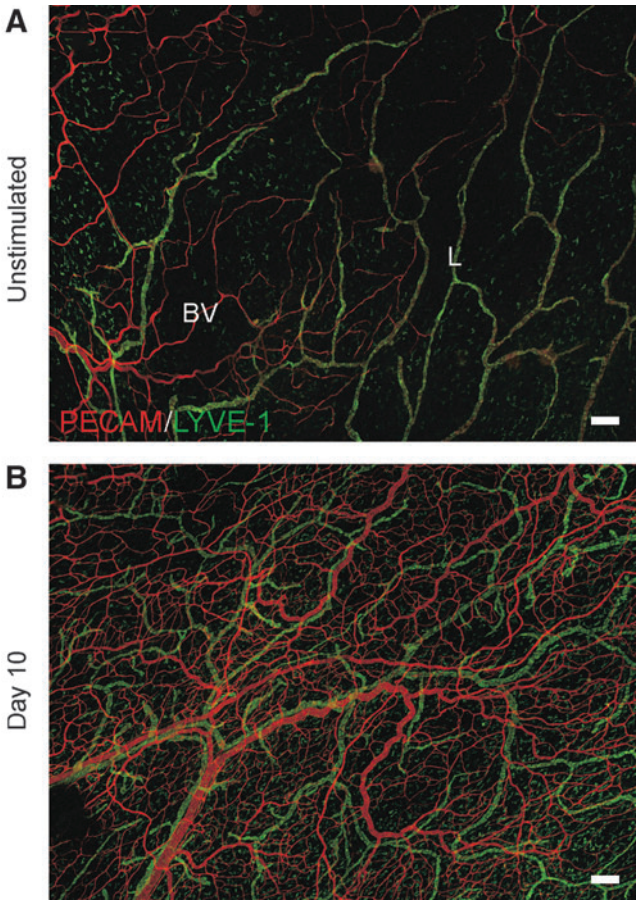

FIG. 1. Representative montages of mesenteric microvascular networks from **(A)** unstimulated and **(B)** compound 48/80-stimulated rats. Immunolabeling for PECAM (*red*) and LYVE-1 (*green*) identified the hierarchies of branching blood vessel (BV) and lymphatic (L) networks. Evidence for angiogenesis and lymphangiogenesis by day 10 is supported by a dramatic increase in vessel density for both blood and lymphatic vessel networks. Scale bars = 200 μm.

Lymphatic/blood endothelial cell connections increase during lymphatic sprouting

Previous work in our laboratory identified the presence of nonluminal lymphatic/blood endothelial cell connections at

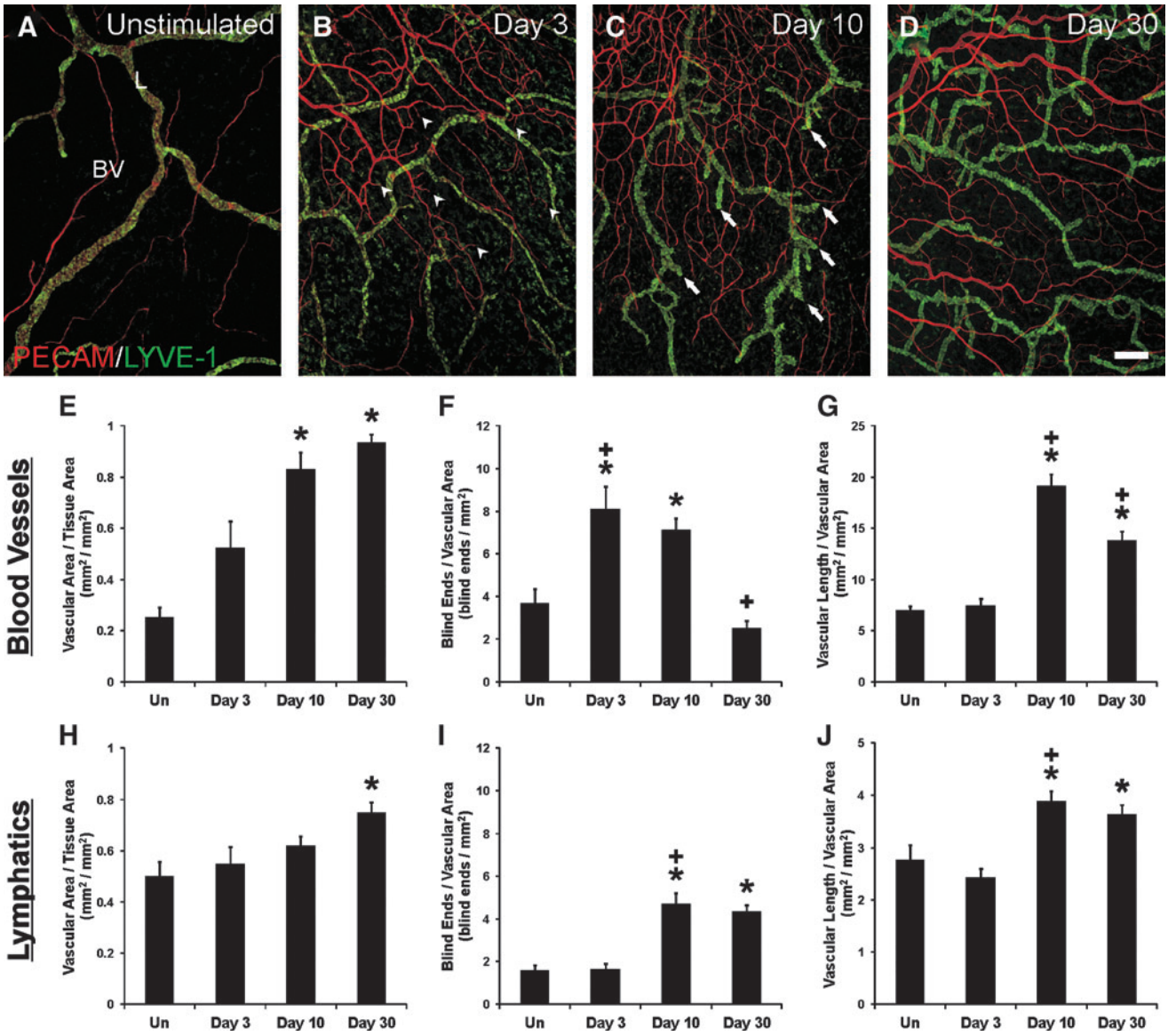

FIG. 2. Compound 48/80-induced inflammatory angiogenesis and lymphangiogenesis in rat mesenteric microvascular networks. **(A–D)** Representative images over the time course of stimulation. Immunolabeling for PECAM (*red*) and LYVE-1 (*green*) identified the hierarchies of branching blood vessel (BV) and lymphatic (L) networks. Increased blood capillary sprouting is observed by 3 days after stimulation (*arrowheads*), while lymphatic sprouting is increased by 10 days after stimulation (*arrows*). Scale bar = 200 μm. **(E–J)** Quantification of angiogenesis and lymphangiogenesis in unstimulated mesenteric microvascular networks (Un) and at 3, 10, and 30 days post stimulation. Blood and lymphatic networks were quantified based on PECAM or LYVE-1 immunolabeling, respectively. **(E, H)** Total vascular area per tissue area. **(F, I)** Number of blind-ended vessel segments per vascular area. **(G, J)** Total vascular length per vascular area. * represents a significant difference compared to the unstimulated control group ($p < 0.05$). + represents a significant difference compared to the previous time point ($p < 0.05$). Values are means ± SEM.

the capillary level in unstimulated rat mesenteric microvascular networks.[10] Apparent connections between lymphatic and blood endothelial cells were defined by continuous PECAM junctional labeling across vessel types.[10] The initial observations of lymphatic/blood endothelial cell connections motivate two questions: 1) Can the occurrence of connections be influenced by their local environment? and 2) Do connections become functional during remodeling scenarios? At day 10 post inflammatory stimulation, the number of connections was significantly increased compared to unstimulated controls (Fig. 6C). Continuous PECAM labeling at sites of connection was confirmed with sub 0.5 μm confocal optical sections (Fig. 6B). The original characterization of these connections in unstimulated tissues demonstrated that connections were between endothelial cells distal to the lumens along a blood capillary sprout.[10] At day 10 post stimulation, lymphatic/blood connections were also located distal to the extent of blood capillary perfusion (Fig. 6D–6F). The injection of FITC-conjugated fixable 40 kDa dextran via the femoral artery identified the hierarchy of stimulated blood microvascular networks including capillary sprouts, but did not identify lymphatic capillaries.

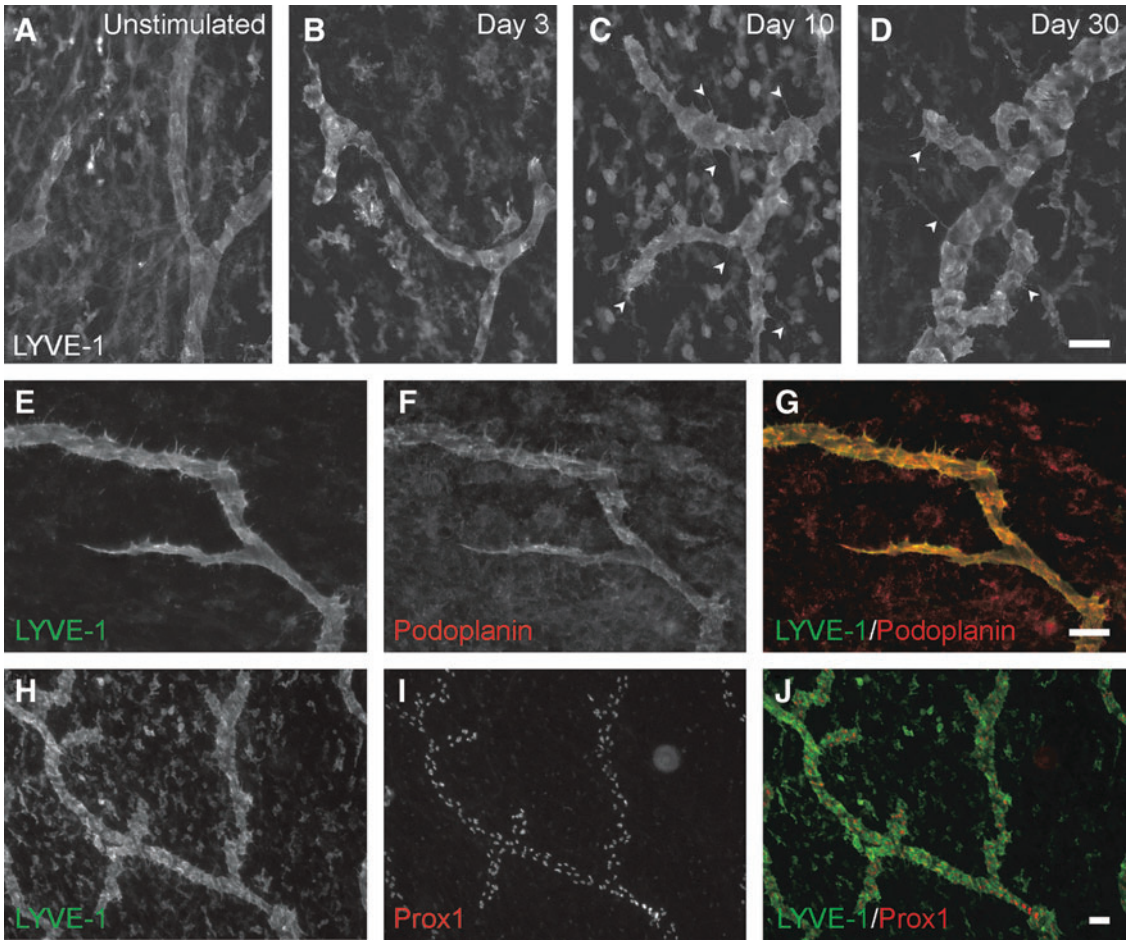

FIG. 3. Characterization of lymphatic vessels in response to compound 48/80 stimulation. **(A–D)** Examples of lymphatic vessel morphologies over the time course of stimulation. LYVE-1 immunolabeling identifies filopodial extensions (*arrowheads*) 10 and 30 days after stimulation. **(E–G)** Examples of lymphatic vessels at day 10 post stimulation co-labeled for LYVE-1 (*green*) and podoplanin (*red*). **(H–J)** Examples of lymphatic vessels at day 10 post stimulation co-labeled for LYVE-1 (*green*) and Prox1 (*red*). Scale bars = 50 μm.

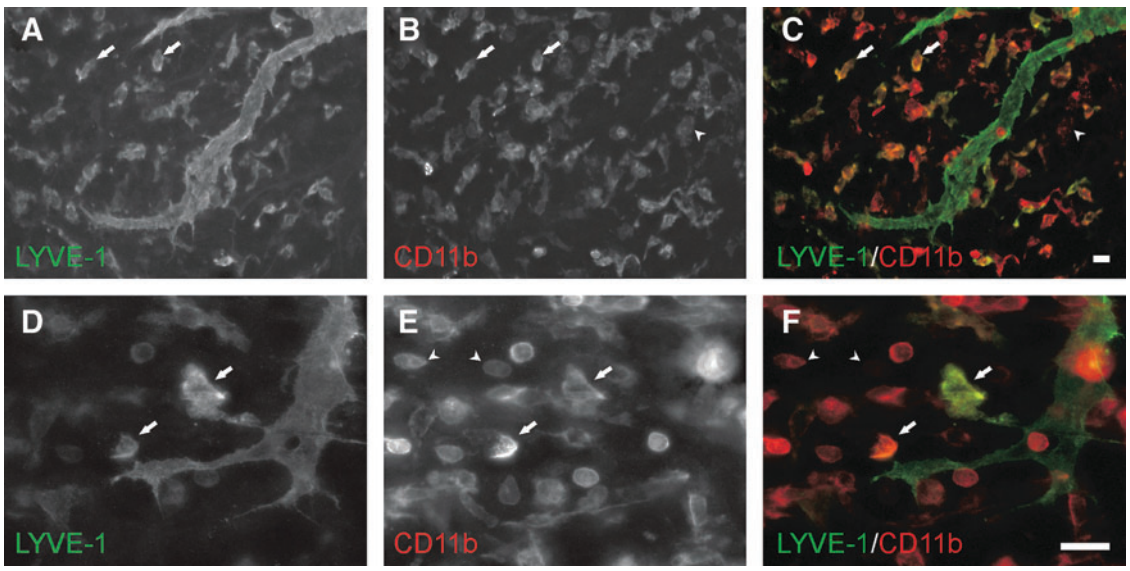

FIG. 4. Identification of macrophages expressing LYVE-1 post compound 48/80 stimulation. Day 10 tissues were immunolabeled for LYVE-1 (*green*) and CD11b (*red*). *Arrows* identify LYVE-1$^+$/CD11b$^+$ cells. *Arrowheads* identify LYVE-1$^-$/CD11b$^+$ cells. Images were captured at 20× **(A–C)** or 60× **(D–F)** magnification. Scale Bars = 20 μm.

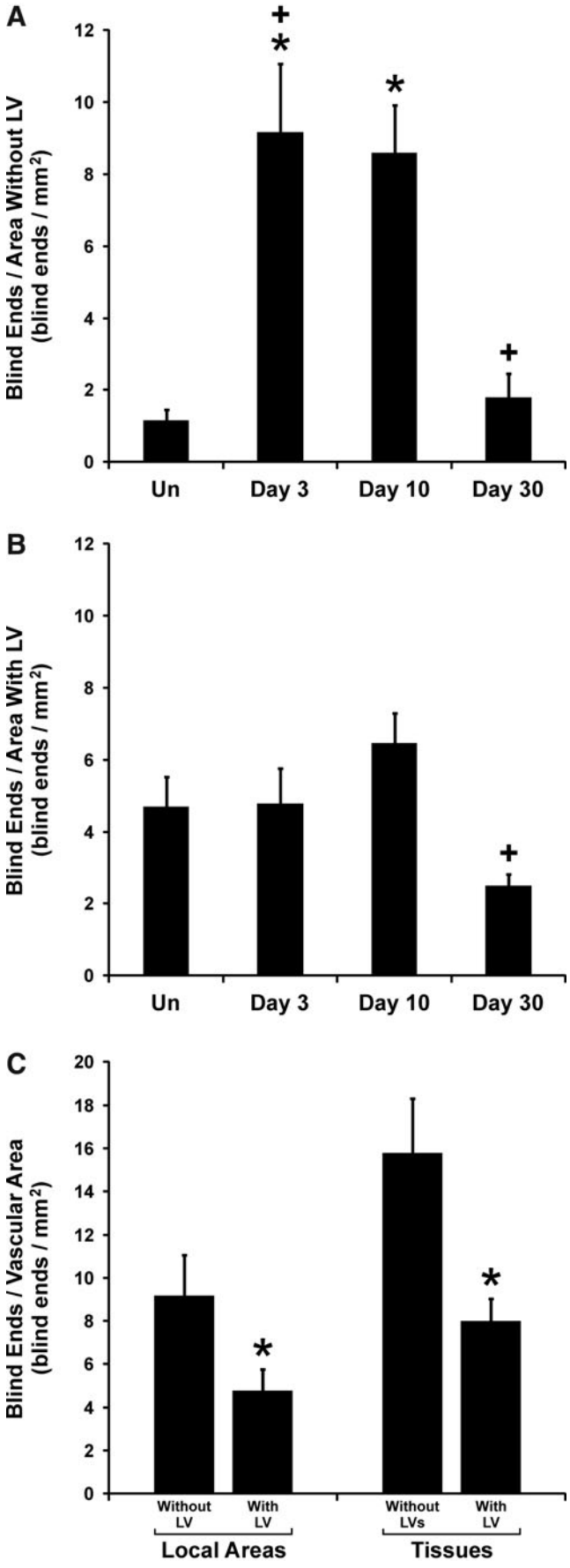

Class III β-tubulin identifies lymphatic blind ends during lymphangiogenesis

We recently reported that class III β-tubulin was transiently upregulated by vascular pericytes during angiogenesis in rat mesenteric microvascular networks[12] and that vascular pericytes are present on a subset of lymphatic capillary sprouts.[10] Based on these observations, we hypothesized that class III β-tubulin transiently identified pericytes along lymphatic sprouts during lymphatic growth associated with inflammation. In compound 48/80 stimulated tissues, class III β-tubulin did not identify pericytes along LYVE-1 positive lymphatic vessels. However, class III β-tubulin positive labeling did identify a subset of lymphatic endothelial cells at day 10 and day 30 (Fig. 7). Labeling was prominent along distal blind-ended vessels and became nonobservable along more proximal segments. Lymphatic endothelial cell-specific labeling was confirmed by comparison of relative spatial localization to PECAM positive cell junctional labeling in optical sections obtained from confocal imaging (Fig. 7). Class III β-tubulin positive lymphatic vessels also co-labeled with lymphatic endothelial cell markers, LYVE-1 and Prox-1(Fig. 8). These observations implicate a possible lymphatic endothelial cell phenotype temporally correlated with lymphangiogenesis. At the time points when class III β-tubulin labeling was observed along lymphatic vessels, labeling of pericytes along blood vessels was less frequent (Fig. 7). This observation is consistent with our previous discovery of class III β-tubulin pericyte expression.[12] At day 3 post 48/80 stimulation when angiogenesis initially peaks, class III β-tubulin is upregulated by perivascular cells along arterioles, venules, and capillaries.[12] At later time points, the percentage of vessels with positive labeling decreases toward the unstimulated scenario.

Discussion

The primary findings of this study are that 1) lymphangiogenesis lags angiogenesis in adult rat mesenteric microvascular networks during inflammation, 2) the presence of lymphatic vessels can attenuate blood capillary sprouting, 3) the occurrence of lymphatic/blood endothelial cell connections can be influenced by their local environment, and 4) lymphatic endothelial cells undergo phenotypic changes at time points associated with lymphangiogenesis. These results emphasize the need to investigate the mechanistic interrelationships between lymphangiogenesis and angiogenesis over the time course of microvascular network growth.

FIG. 5. The effect of lymphatic vessel presence on angiogenesis in unstimulated mesenteric microvascular networks (Un) and at 3, 10, and 30 days post stimulation. **(A)** The number of blood capillary sprout blind ends in local areas containing no lymphatic vessels (LV). **(B)** The number of blood capillary sprout blind ends in local areas with lymphatic vessels. * represents a significant difference compared to the unstimulated control group ($p < 0.05$). + represents a significant difference compared to the previous time point ($p < 0.05$). **(C)** Comparison between the number of blood capillary sprout blind ends at 3 days post stimulation in local tissue areas with and without lymphatic vessels (*left*) or in entire tissues with or without lymphatic vessels (*right*). * represents a significant difference between groups ($p < 0.05$). Values are means ± SEM.

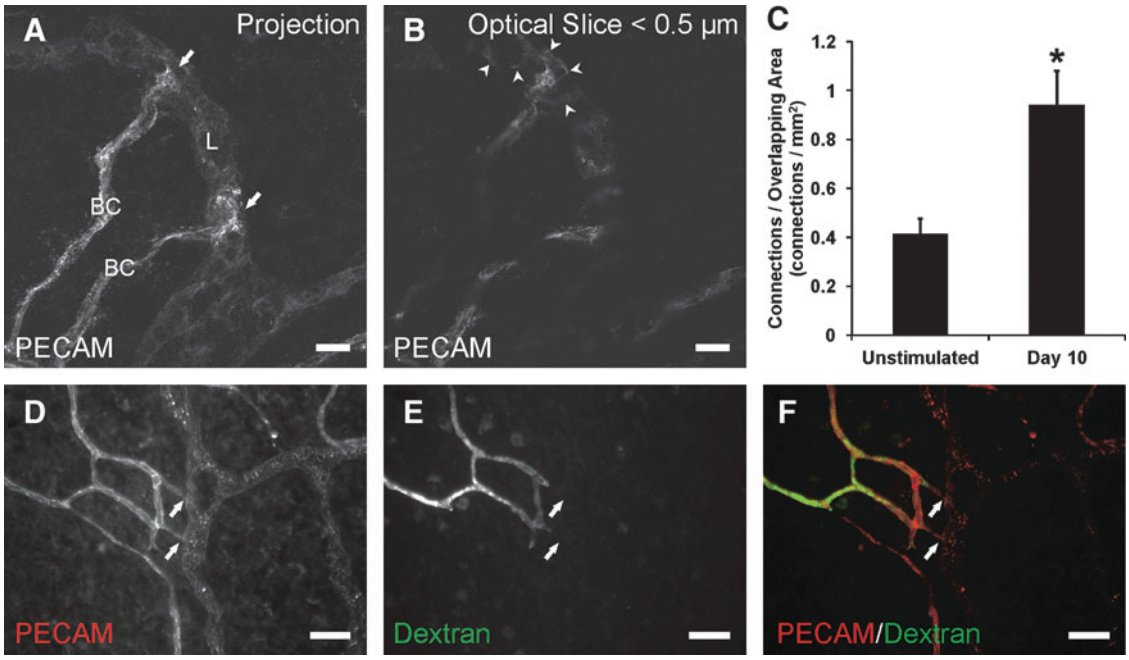

FIG. 6. Lymphatic/blood endothelial cell connections during peak lymphatic sprouting. **(A)** Confocal projection of endothelial cell connections (*arrows*) between blood capillaries (BC) and lymphatic vessels (L) identified by PECAM immunolabeling at day 10. **(B)** Sub 0.5 μm confocal optical slice indicating continuous PECAM labeling along blood and lymphatic endothelial cell junctions (*arrowheads*). **(C)** Quantification of the number of apparent lymphatic/blood endothelial cell connections per overlapping blood and lymphatic vascular area. * represents a significant difference between groups ($p < 0.05$). Values are means ± SEM. **(D–F)** Intravenous injection of fixable FITC-dextran identified the lumens of blood vessels and capillary sprouts. The presence of dextran terminated along capillary sprouts proximal to endothelial cell connections (*arrows*). Scale bars = **(A** and **B)** 20 μm; **(D–F)** 50 μm.

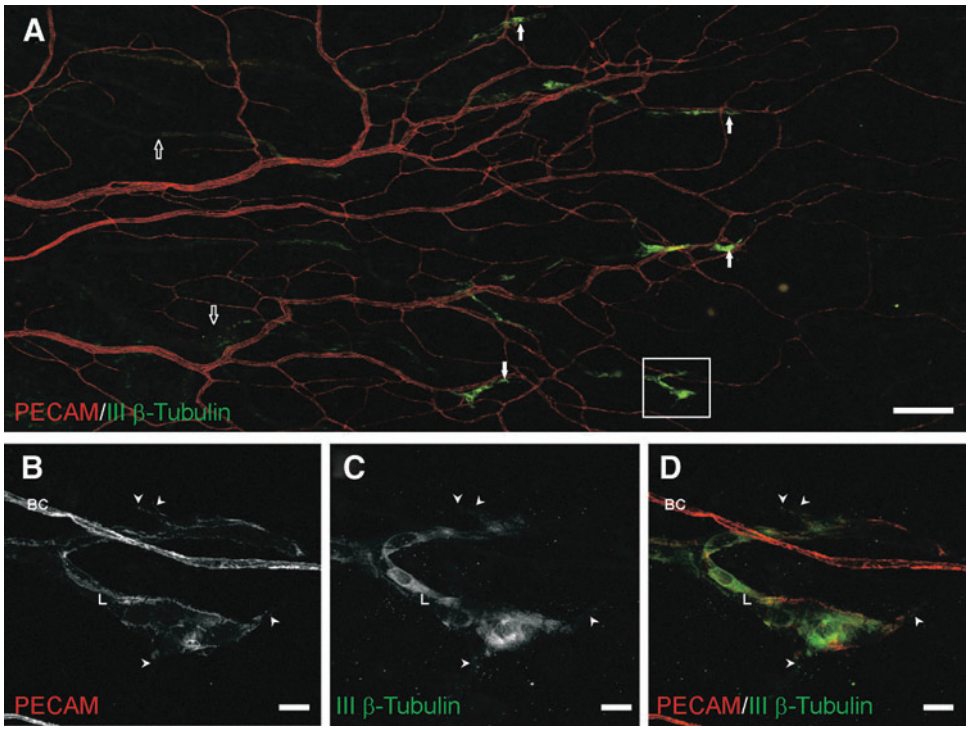

FIG. 7. Class III β-tubulin expression by lymphatic blind ends during peak lymphatic sprouting. Immunolabeling of PECAM (*red*) and class III β-tubulin (*green*) identified distal ends of lymphatic capillaries, resembling lymphatic sprouts. **(A)** A representative microvascular network 30 days post-stimulation labeled for PECAM (*red*) and class III β-tubulin (*green*). Class III β-tubulin identified distal lymphatic segments (*white arrows*). Blood vessels and proximal lymphatic vessels (*open arrows*) did not label positively for class III β-tubulin. **(B–D)** Confocal projection from the outlined box in **(A)** confirming the co-localization of PECAM and class III β-tubulin labeling on endothelial cells of lymphatic vessels (L), but not blood capillaries (BC). Lymphatic capillaries expressing class III β-tubulin commonly contained filopodia extensions (*arrowheads*). Scale bars = **(A)** 200 μm; **(B–D)** 20 μm.

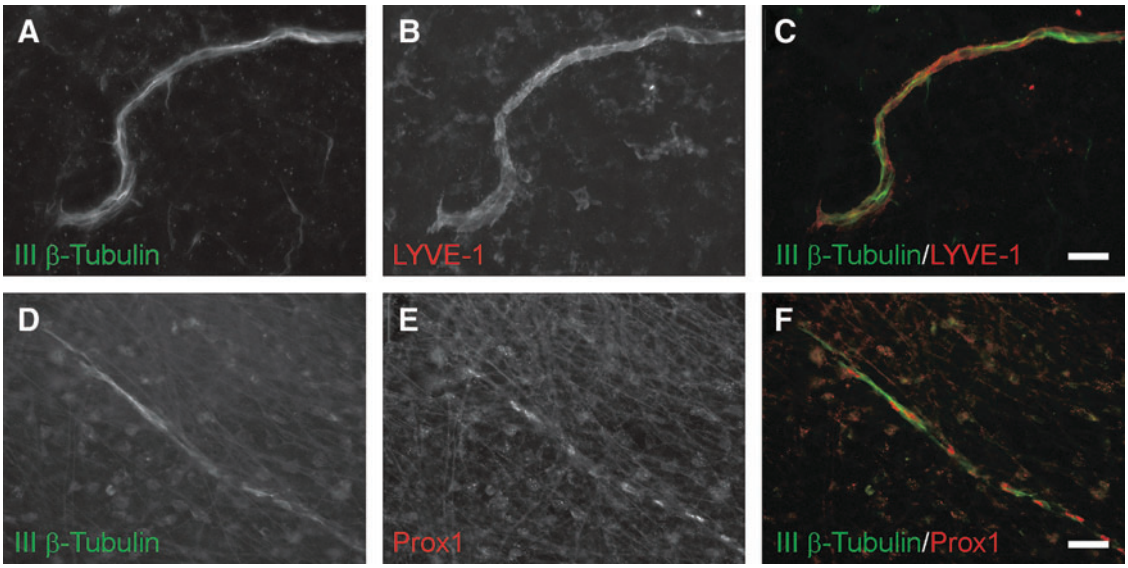

FIG. 8. Representative lymphatic vessels at day 10 post stimulation co-labeled for class III β-tubulin (*green*) and lymphatic markers (*red*), LYVE-1 **(A–C)** and Prox1 **(D–F)**. Scale bars = 50 μm.

The compound 48/80 stimulus used for this study has been previously shown to cause histamine release by mast cells and produces a robust microvascular network growth response in the rat mesentery characterized by increases in vascularized area, capillary sprouting, and vascular length density.[8,9] Our current results demonstrate this response and additionally show that compound 48/80 stimulation causes lymphangiogenesis marked by analogous increases in lymphatic network size, sprouting, intussusceptive loop formation, and vessel length density over a similar time course. Evidence for lymphangiogenesis lagging angiogenesis is supported by lymphatic capillary sprouting increasing at day 10 versus day 3 for blood vessels. This delay in sprouting results in a delay in lymphatic versus blood vascular network area enlargement. This temporal relationship between angiogenesis and lymphangiogenesis is supported by similar descriptions in other models.[2,13,14] Baluk et al. demonstrated that increases in lymphatic area density followed blood vessel remodeling in chronic airway inflammation.[13] They also observed that the lymphatic network persists compared to blood microvascular networks after the inflammation resolved. This is consistent with our observations of a sustained increase in lymphatic vessel density versus a regression in blood vessel density at day 30.

Our quantification of angiogenesis and lymphangiogenesis utilized previously established angiogenic metrics.[7,12,15] Capillary sprouting was evaluated by quantifying the number of blind-ended capillary segments per vessel type. For the blood microvasculature in the mesentery, such blind-ended vessels are associated with endothelial cell proliferation.[5] While we cannot rule out that some blind-ended vessels might be undergoing regression, the overall effect of an increase in their number leads increases in blood microvascular network area and length density. Thus, blood capillary blind ends can be assumed to be indicative of sprouting and angiogenesis. Since lymphatic networks are open loop systems, the number of lymphatic blind-ended vessels is not necessarily indicative of lymphangiogenesis. Rather lymphangiogenesis is indicated by an increase in the number of lymphatic blind ends from one time point to another. The increase in the number of lymphatic blind ends from day 3 to day 10 post stimulation provides evidence for lymphangiogenesis. Lymphangiogenesis at day 10 is further supported by the presence of lymphatic endothelial filopodia extensions, which have been previously documented as an indicator of lymphatic growth.[13,16] The lack of change in lymphatic blind ends from day 10 to day 30 suggests that the increase in lymphatic sprouting observed from day 3 to day 10 may not persist.

Recently, lymphatic and blood endothelial cells have been shown to share multiple growth mechanisms.[17] The common expression of growth factor receptors[18] suggests that lymphatic and blood endothelial cells might compete for the same local growth factors. Benest et al. demonstrated that the presence lymphatic networks attenuated VEGF-C induced angiogenesis.[4] Our results further demonstrate this relationship in a multi-factorial inflammatory scenario and motivate future investigations aimed at elucidating the mechanistic interplay between lymphatic and blood endothelial cells.

The importance of interactions between lymphatic and blood endothelial cells was recently highlighted by our laboratories description of nonluminal lymphatic/blood endothelial cell connections in unstimulated adult rat mesenteric microvascular networks. This finding challenged the classical view that blood and lymphatic microvascular networks are distinct systems without direct interaction.[2,19,20] The possibility of mispatterning between systems is supported by the presence of blood-filled lymphatic vessels in Prox1 conditional mutant mice.[21] Johnson et al. observed that Prox1 inhibition via siRNA *in vitro* resulted in a change from lymphatic to blood endothelial cell phenotype.[21] Their work suggests that local epigenetic environments are sufficient to modulate lymphatic/blood endothelial cell interactions. In our study, we provide evidence that a local change in the environment associated with our inflammatory model can cause an increase in lymphatic/blood endothelial cell connections. The increase in connections was observed 10 days

after stimulation with compound 48/80. The majority of these connections were blind-ended blood capillary sprouts interacting with lymphatic vessels (data not shown). Since capillary sprout density in areas vascularized by blood and lymphatic vessels remained unchanged over the time course of inflammation, we speculate that the increase in lymphatic/blood connections is a result of environmental changes rather than an increased probability associated with angiogenesis. The function of the physical interactions remains unclear, yet our results do indicate that they are dynamic and implicate the rat mesentery as a model for investigating signaling molecules involved in lymphatic/blood system mispatterning.

The characterization of the cellular dynamics across the time course of angiogenesis in the rat mesentery has identified specific endothelial cell and pericyte phenotypes temporally linked to capillary sprouting.[7,12,22] Here we demonstrate the usefulness of this approach to identify novel lymphatic endothelial cell phenotypes associated with lymphangiogenesis. Class III β-tubulin is a cytoskeletal protein that forms heterodimers with α-tubulins during microtubule assembly.[23] In normal tissues, it is expressed almost exclusively in glial and neural progenitor cells in the central nervous system and nerves in the peripheral nervous system.[23,24] Class III β-tubulin expression has also been reported in lymphatic and venous valves.[25] Recently, transient class III β-tubulin expression was documented in perivascular cells during angiogenesis.[12] In this study, we observed class III β-tubulin expression along distal ends of terminal blind-ended lymphatic capillaries during lymphangiogenesis. Positive labeling by lymphatic endothelial cells was confirmed based on a relative labeling pattern compared to PECAM and co-labeling with Prox1. Additionally, in our laboratory co-labeling of remodeling mesenteric tissues with PECAM and NG2 confirms that the initial lymphatic vessels with similar morphologies to those expressing class III β-tubulin lack perivascular cell wrapping. While the function of this marker is unclear, our observations motivate a future area of research focused on understanding how lymphatic endothelial cells differ at different locations along a lymphatic network during lymphangiogenesis. Lymphatic endothelial cell expression of class III β-tubulin also serves as an example of phenotypic overlap across neural, blood, and lymphatic cell types.

In summary, our study shows that lymphangiogenesis lags angiogenesis over the time course of microvascular network growth in adult mesenteric microvascular networks in response to an inflammatory stimulation and that the presence of lymphatic vessels can attenuate capillary sprouting. These results, coupled with the observations of increased lymphatic/blood endothelial cell connections and class III β-tubulin upregulation during lymphatic growth, highlight the importance for future investigations to be aimed at understanding how angiogenesis and lymphangiogenesis are mechanistically interrelated.

Author Disclosure Statement

This work was supported by the Board of Regents of the State of Louisiana LEQSF(2009-12)-RD-A-19 (PI: WL Murfee) and the Tulane Center for Aging funded by NIH grant P20GM103629-01A1 (PI: M Jazwinski).

References

1. Mouta C, Heroult M. Inflammatory triggers of lymphangiogenesis. Lymphat Res Biol 2003;1:201–218.
2. Clark ER, Clark EL. Observations on living mammalian lymphatic capillaries—Their relation to the blood vessels. Am J Anat 1937;60:253–298.
3. Baluk P, Fuxe J, Hashizume H, Romano T, Lashnits E, Butz S, Vestweber D, Corada M, Molendini C, Dejana E, McDonald DM. Functionally specialized junctions between endothelial cells of lymphatic vessels. J Exp Med 2007;204:2349–2362.
4. Benest AV, Harper SJ, Herttuala SY, Alitalo K, Bates DO. VEGF-C induced angiogenesis preferentially occurs at a distance from lymphangiogenesis. Cardiovasc Res 2008;78:315–323.
5. Kelly-Goss M, Winterer E, Stapor P, Yang M, Sweat R, Stallcup W, Schmid-Schonbein G, Murfee W. Cell proliferation along vascular islands during microvascular network growth. BMC Physiol 2012;0:7.
6. Stapor PC, Murfee WL. Spatiotemporal distribution of neurovascular alignment in remodeling adult rat mesentery microvascular networks. J Vasc Res 2012;49:299–308.
7. Murfee WL, Rehorn MR, Peirce SM, Skalak TC. Perivascular cells along venules upregulate NG2 expression during microvascular remodeling. Microcirculatio. 2006;13:261–273.
8. Franzen L, Ghassemifar R, Malcherek P. Experimental mast cell activation improves connective tissue repair in the perforated rat mesentery. Agents Actions 1991;33:371–377.
9. Norrby K, Jakobsson A, Sorbo J. Mast-cell-mediated angiogenesis: A novel experimental model using the rat mesentery. Virchows Arch B Cell Pathol Incl Mol Pathol 1986;52:195–206.
10. Robichaux JL, Tanno E, Rappleye JW, Ceballos M, Stallcup WB, Schmid-Schonbein GW, Murfee WL. Lymphatic/blood endothelial cell connections at the capillary level in adult rat mesentery. Anat Rec (Hoboken) 2010;293:1629–1638.
11. Murfee WL, Rappleye JW, Ceballos M, Schmid-Schonbein GW. Discontinuous expression of endothelial cell adhesion molecules along initial lymphatic vessels in mesentery: The primary valve structure. Lymphat Res Biol 2007;5:81–89.
12. Stapor PC, Murfee WL. Identification of class III beta-tubulin as a marker of angiogenic perivascular cells. Microvasc Res 2012;83:257–262.
13. Baluk P, Tammela T, Ator E, Lyubynska N, Achen MG, Hicklin DJ, Jeltsch M, Petrova TV, Pytowski B, Stacker SA, Yla-Herttuala S, Jackson DG, Alitalo K, McDonald DM. Pathogenesis of persistent lymphatic vessel hyperplasia in chronic airway inflammation. J Clin Invest 2005;115:247–257.
14. Nakao S, Zandi S, Hata Y, Kawahara S, Arita R, Schering A, Sun D, Melhorn MI, Ito Y, Lara-Castillo N, Ishibashi T, Hafezi-Moghadam A. Blood vessel endothelial VEGFR-2 delays lymphangiogenesis: An endogenous trapping mechanism links lymph- and angiogenesis. Blood 2011;117:1081–1090.
15. Yang M, Aragon M, Murfee WL. Angiogenesis in mesenteric microvascular networks from spontaneously hypertensive versus normotensive rats. Microcirculation 2011;18:574–582.
16. Gerhardt H, Golding M, Fruttiger M, Ruhrberg C, Lundkvist A, Abramsson A, Jeltsch M, Mitchell C, Alitalo K, Shima D, Betsholtz C. VEGF guides angiogenic sprouting utilizing endothelial tip cell filopodia J Cell Biol 2003;161:1163–1177.
17. Adams RH, Alitalo K. Molecular regulation of angiogenesis and lymphangiogenesis Nat Rev Mol Cell Biol 2007;8:464–478.

18. Lohela M, Bry M, Tammela T, Alitalo K. VEGFs and receptors involved in angiogenesis versus lymphangiogenesis. Curr Opin Cell Biol 2009;21:154–165.
19. Hauck G. Functional aspects of the topical relationship between blood capillaries and lymphatics of the mesentery. Pflugers Arch 1973;339:251–256.
20. Schmid-Schoenbein GW, Zweifach BW, Kovalcheck S. The application of stereological principles to morphometry of the microcirculation in different tissues. Microvasc Res 1977;14: 303–317.
21. Johnson NC, Dillard ME, Baluk P, McDonald DM, Harvey NL, Frase SL, Oliver G. Lymphatic endothelial cell identity is reversible and its maintenance requires Prox1 activity. Genes Dev 2008;22:3282–3291.
22. Anderson CR, Hastings NE, Blackman BR, Price RJ. Capillary sprout endothelial cells exhibit a CD36 low phenotype: Regulation by shear stress and vascular endothelial growth factor-induced mechanism for attenuating anti-proliferative thrombospondin-1 signaling. Am J Pathol 2008;173:1220–1228.
23. Katsetos CD, Legido A, Perentes E, Mork SJ. Class III beta-tubulin isotype: A key cytoskeletal protein at the crossroads of developmental neurobiology and tumor neuropathology. J Child Neurol 2003;18:851–866; discussion 867.
24. Draberova E, Del Valle L, Gordon J, Markova V, Smejkalova B, Bertrand L, de Chadarevian JP, Agamanolis DP, Legido A, Khalili K, Draber P, Katsetos CD. Class III beta-tubulin is constitutively coexpressed with glial fibrillary acidic protein and nestin in midgestational human fetal astrocytes: Implications for phenotypic identity. J Neuropathol Exp Neurol 2008;67:341–354.
25. Kang J, Lee I. TuJ1 (class III beta-tubulin) as phenotypic marker of lymphatic and venous valves. Cardiovasc Pathol 2006;15:218–221.

Address correspondence to:
Walter L. Murfee, Ph.D.
Lindy Boggs Center, Suite 500
Department of Biomedical Engineering
Tulane University
New Orleans, LA 70118

E-mail: wmurfee@tulane.edu